

Tools for Assessment and Planning of Aquaculture Sustainability



SHORT TITLE:

TAPAS

COORDINATOR:

Prof. Trevor Telfer

ORGANISATION:

University of STIRLING, UK

TOPIC:

H2020- SFS-11b-2015

PROJECT NUMBER:

678396

DELIVERABLE: D7.6

Automatic in-situ measurement systems report

Contributing Authors:

Manolis Ntoumas, HCMR

Manolis Tsapakis, HCMR

Nikos Papandroulakis, HCMR

Vagelis Chalkiadakis, HCMR

Marnix Laanen, WI



Ver	Date	Changes	Author
1	29/11/2019	Preliminary draft (Draft0)	HCMR
2	9/12/2019	Final Draft	HCMR
3	11/12/2019	Final Document for submission	HCMR
4			
5			



Summary

WP 7 is focused on improving existing and developing new integrated operational tools for the timely and cost-efficient monitoring of aquaculture production.

In this deliverable the development of new in situ observation technologies of physical, ecological and chemical water quality including novel biosensors and optical sensors as well as monitoring the integrity of the cage material is presented. The document provides the detailed description and their testing and validation procedure of three systems developed within TAPAS:

- An Aquaculture Specific Profiler that carries out vertical profiles of the water from the surface to the bottom of the fish farm, with user configurable payload
- An Autonomous Underwater Vehicle that is able to perform regular inspections of the cage material condition and transmits alarms in case of problems detection
- An optical sensors based observation system providing ecological water quality measurements by recording radiance and irradiance and performs continuous and autonomous high-quality measurements for water quality monitoring and satellite validation



Table of Contents

Summary	3
Table of Contents	4
1 Introduction	6
2 Aquaculture Specific Profiler	8
2.1 Introduction	8
2.2 Monitoring concept	8
2.3 System components.....	9
2.3.1 ASP Variable Buoyancy System	9
2.3.2 VBS operation	10
2.3.3 VBS pump	10
2.3.4 VBS Bladder.....	11
2.3.5 ASP hydraulic circuit.....	11
2.3.6 ASP housing.....	12
2.3.7 ASP control board	12
2.3.8 ASP navigation	13
2.4 ASP housing and variable buoyancy laboratory testing	14
2.4.1 Housing testing	14
2.4.2 VBS testing	15
2.5 ASP housing and variable buoyancy field testing	15
3 Autonomous underwater vehicle	17
3.1 Introduction	17
3.2 Monitoring concept and System Description	17
3.2.1 AUV – Vehicle and Sensors	18
3.2.2 Conversion of the ROV to AUV	18
3.2.3 Optical Navigation.....	19
3.2.4 Optical Net Inspection s/w.....	20
3.2.5 Docking-station	22
3.2.6 Implementation of the wireless Charging system	22
3.2.7 Docking procedure software implementation.....	23
3.3 Trials of the AUV System in the fish-cage test facility	24



4	Autonomous above water radiometer system WISPstation	27
4.1	Monitoring concept	27
4.2	System description.....	29
4.2.1	Database and output API	32
4.3	Operational deployment.....	32
4.3.1	Deployment at Souda Bay, Crete (Greece)	32
4.3.2	Deployment at Hungary	34
4.4	Example WISPstation results	35
4.5	System performance.....	37
4.6	Link to TAPAS DST (recommendations for wider use)	37
5	Closing Remarks	38
6	References	39



1 Introduction

As fish farms increase in size and complexity, the size and designs of fish cages evolve, and new location types are taken into use, more sophisticated technological solutions will be required to provide sufficient knowledge and information to monitor and/or control the production process. Moreover, as the scale of production increases, so does the likelihood that the industry will face emerging biological, economic and social challenges that may influence the ability to maintain ethically sound, productive and environmentally friendly production of fish. The Precision Fish Farming concept [1] aims at applying engineering principles to Aquaculture, improving the farmer's ability to monitor, control and document the processes in fish farms. This can be achieved through increased use of emerging technologies and automated systems. Using technology to automate the regular daily operations could lead to vast process improvements and operational costs reductions.

Contributing to the above objective, the key objective of Task 7.2 (Novel real time in situ measurement systems) is to deploy existing and develop new innovative systems for automatic in-situ measurements of physical, ecological and chemical water quality, including innovative biosensors and optical sensors as well as monitoring the integrity of the cage material.

In this framework, three systems were developed, tested and operated in operational conditions at selected sites:

- Aquaculture Specific Profiler (ASP)
- Autonomous Underwater Vehicle (AUV)
- WISPstation

All three systems are going to improve the awareness level of the farmer in relation to the infrastructure's condition and to the quality of the water, and require minimal human intervention to their operation, as they have been designed with functional and energy autonomy in mind. In this way, several costly and labor intensive operations will be automated and will require less resources and capital, increasing thus the profit margins.

An Aquaculture Specific Profiler capable of performing vertical profiles from the surface down to the depth of fish farm cages has been implemented. The payload is user configurable and the profiler is able to host several sensors measuring all key environmental parameters of the seawater and/or underwater camera modules in order to inspect underwater structures and components. Data transmission is near real time through GPRS/3G networking while vertical movements are user configurable.

An Autonomous Underwater Vehicle (AUV) has been developed, implemented and demonstrated in operational environment that monitors the integrity of the cage material, to prevent potential escapees. The AUV has been developed using navigation technologies already used for UAVs (unmanned air vehicle) and UGVs (unmanned ground vehicle), adapted for use in the underwater environment. Extensive testing and a pilot demonstration was performed at the Aquaculture facility of HCMR at Souda Bay, Crete



A novel optical sensors based system was built and deployed that provides cost-efficient observations of ecological water quality and supports integration of in situ observations with moderate and high-resolution satellite imagery.

This document describes the details of the abovementioned systems, their capabilities, and the results of their pilot operation.



2 Aquaculture Specific Profiler

2.1 Introduction

Coastal profiling systems can help to integrate indispensable information on water column characteristics in coastal areas. The most mature system technology used extensively in oceanography worldwide, are the ARGO type profiling floats. Despite the maturity of this technology and the successful operations in the open sea, the ARGO floats are still used sparingly in coastal profiling. Besides the proven technology, fixed (at the surface or bottom) profilers are also under development in projects like JERICO-NEXT and worldwide. The majority of the systems are research prototypes, quite difficult to use and very different in their operation. There are two types of profilers:

- *Buoy profilers* deployed on the sea surface that automatically raise and lower oceanographic instruments at pre-programmed intervals using an on-board winch. A typical buoy profiler consists of a buoyant housing that contains the winch, wire drum, batteries, and communications equipment.
- *Bottom mounted profilers* also use an automatic winch but, unlike buoy profilers, the winch is anchored on the bottom and is used to raise oceanographic instrument embedded in a buoyant housing.

The Aquaculture Specific Profiler (ASP) presented hereinafter, aims to monitor the sea column next to the aquaculture facilities. The data will be collected at specific water depths allowing the characterization of the surrounding water mass, with the use of sensors payload. The profiler is based on a Variable Buoyancy System (VBS), using the same principle of operation as the ARGO floats and it is capable to perform vertical profiles from the surface down to 50 meters. It can operate attached on a mooring line performing vertical profiles in a fixed point or deployed without anchoring system and move under the influence of sea currents collecting Lagrangian measurements. The payload is user configurable and the profiler is able to host several sensors measuring environmental parameters of the seawater and/or underwater camera modules in order to inspect underwater structures and components and collect visual data.

2.2 Monitoring concept

The mission concept of the ASP in the TAPAS project is demonstrated in Figure 1. The profiler is attached on a simple mooring line and performs vertical profiles in specific user intervals logging the data internally and transmitting it when it surfaces. The user is able to command the profiler to move with predefined descent/ascent rate in order to achieve the desired vertical resolution of the measured parameters. In addition, the profiler could be stabilized in a specified “parking depth” and collect averaged data for longer periods.

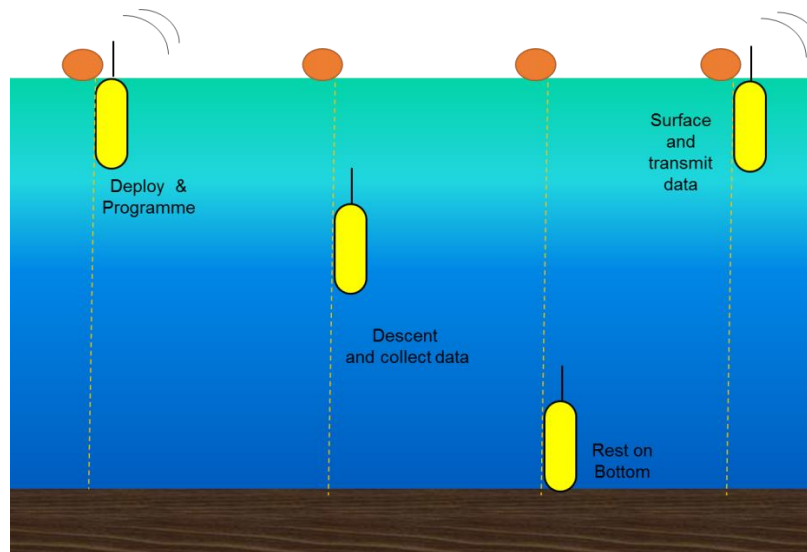


Figure 1: ASP Mission Concept

2.3 System components

2.3.1 ASP Variable Buoyancy System

The Variable Buoyancy System (VBS) system is used to achieve repeatable two-way buoyancy changes by pumping a liquid, usually oil, in and out of pressure housing. To increase buoyancy, oil is pumped from inside the pressure housing to an external flexible bladder. The bladder expands and it displaces water, increasing the buoyant force on the system while the mass remains unchanged. When a decrease in buoyancy is needed, a valve is opened and the surrounding water pressure drives the oil back to the internal housing. The limitation regarding the buoyancy adjustment cycles are limited only by the power availability and the components endurance in the harsh sea environment. The VBS components are placed inside the ASP housing except the external bladder which gives the mechanism the desired negative or positive buoyancy by reducing or increasing its volume, respectively. The change in volume is achieved by a closed hydraulic circuit, which consists of a pump, a non-return valve, a double-acting solenoid valve and an internal oil storage bladder (Figure 2). Hydraulic connection of the above components is achieved by high-pressure hoses while control of pump and solenoid operation is performed by an Arduino micro controller.

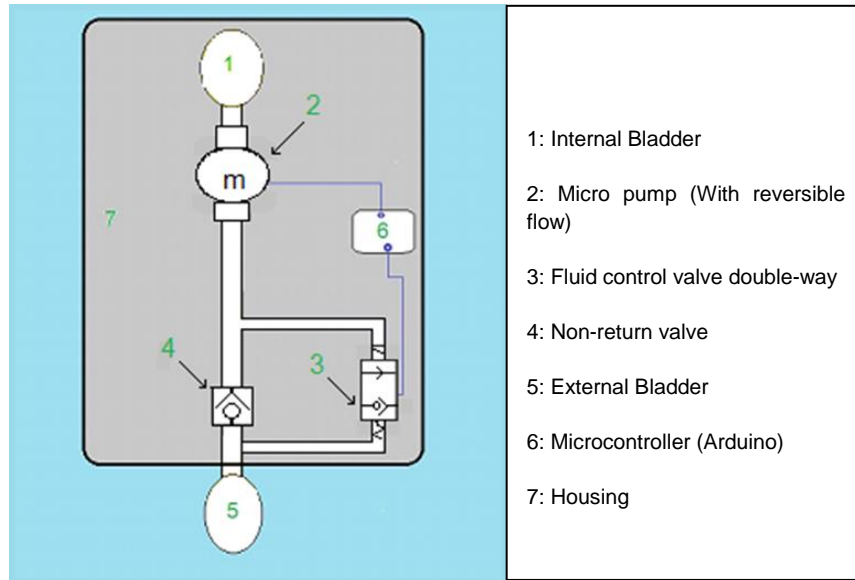


Figure 2: VBS system components

2.3.2 VBS operation

Prior the diving of the device, the outer bladder (5) is filled with oil while the interior is empty, so the mechanism is on the surface. To start the dive, oil must be transferred from the external bladder (5) to the inside bladder (1) to reduce the overall volume of the structure and begin to submerge. The microcontroller (6) activates the pump (2), control the flow direction and open the solenoid valve (3). The non-return valve (4) during diving remains closed and is not used. For the emergence of the profiler, the oil should be led to the outer bladder (5) from the inner bladder (1). Similarly, to diving the microcontroller will give the two commands to the pump, but without having to command the solenoid actuation as it is normally closed. The non-return valve (4) will open due to the oil pressure, resulting in the desired filling of the external bladder (5).

2.3.3 VBS pump

The variable buoyancy mechanism uses a MG 2000 pump (Figure 3) to circulate the oil in its hydraulic circuit. It is a gear technology pump and operates by sucking the hydraulic fluid from the inlet and pressed into the two-pinion outlet. The criteria for selecting the MG2000 for this application are:

- It is able to handle the pressure
- Large range of fluid viscosity
- Smooth flow without pulse
- Made of high corrosion-resistant materials
- Reversible flow
- Small size and weight

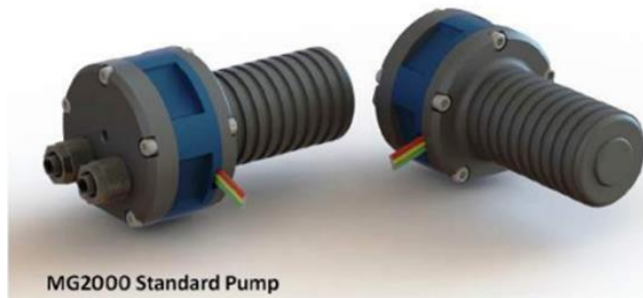


Figure 3: The MG2000 Pump

2.3.4 VBS Bladder

The VBS uses two bladders (flexible containers), one of which is inside the housing while the other is attached below the ASP. With the aid of the pump, 1 liter of hydraulic oil moves controllably from one to the other alternating the overall volume of the ASP. The body of the bladder is not particularly stress-strapped, as the external pressure it receives is balanced by the circuit internal pressure, and so its walls can be relatively thin and therefore flexible.

2.3.5 ASP hydraulic circuit

The rest of the components that are included in the hydraulic circuit of the ASP (Figure 4) are a type 2WX 030 06 F I electromagnetic valve, a passive mechanical non reverse valve, inox connectors and flexible tubing certified to operate under 10 Bar of pressure.

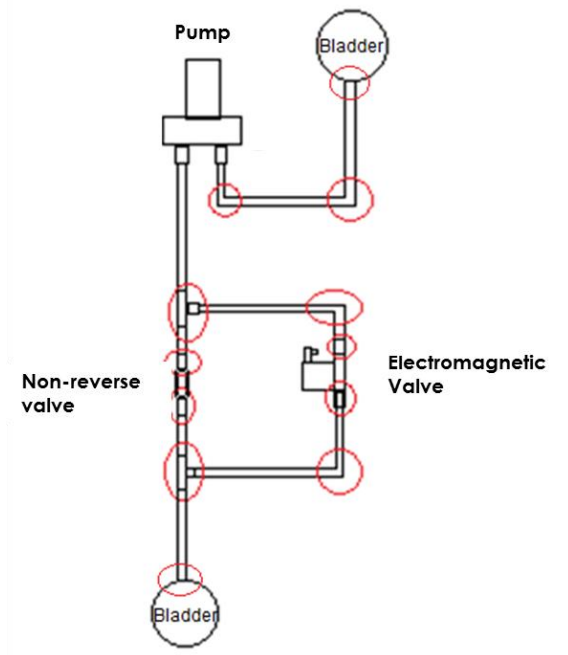


Figure 4: The ASP hydraulic circuit

2.3.6 ASP housing

The ASP cylindrical housing and the two closing lids are made from ACETAL POMC with overall dimensions of 150mm × 120mm × 1000mm. The lids are equipped with underwater connectors in order to host the sensors/scientific payload of the ASP. The whole structure was successfully tested prior to manufacturing for stress analysis, using the *UnderPressure* software package (Figure 5).

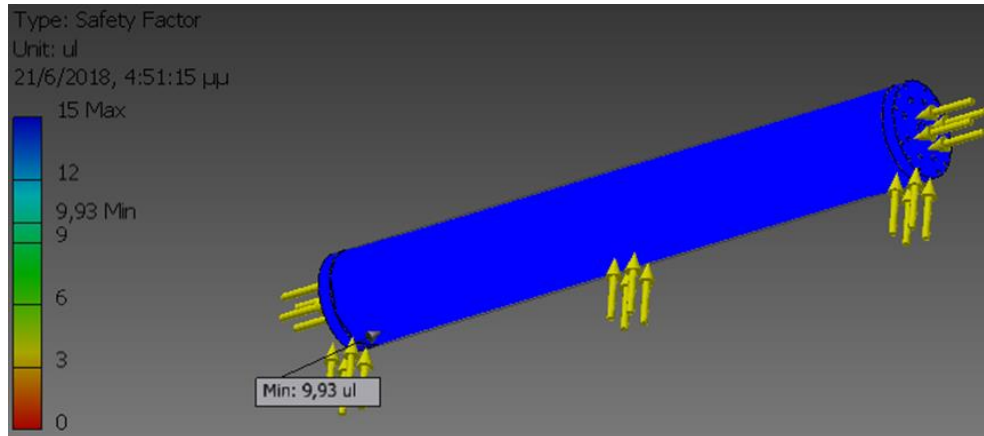


Figure 5: ASP housing stress analysis

2.3.7 ASP control board

Two types of microcontrollers are used in the electronic circuitry of the mechanism. An Arduino Pro Mini is used as master controller which controls the operation of the entire electronic circuit. An Arduino UNO is the secondary controller and it is used to guide the pump and solenoid valve, for the emergence / diving of the mechanism and communicate with a Raspberry Pi that powers the sensors, records their values on an SD Card, creates the mission data files and communicates bi-directionally through the embedded Wi-Fi board (Figure 6).

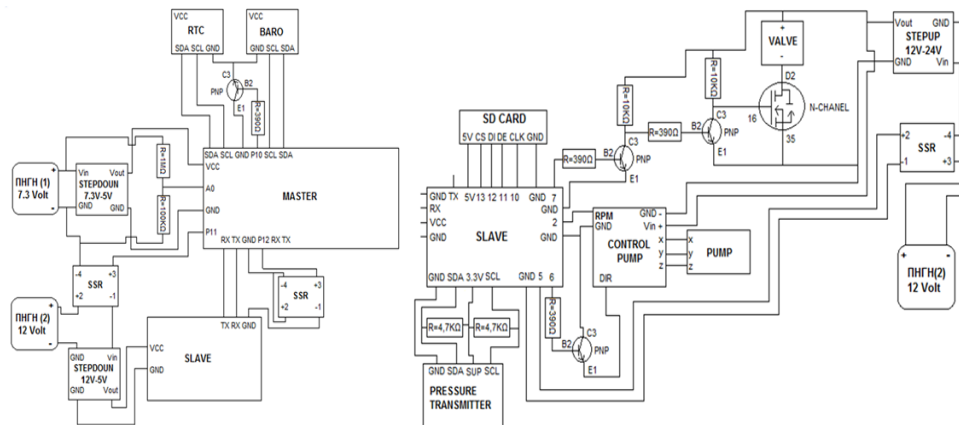


Figure 6: ASP master and slave controller circuit

The power source selected for the master circuit consists of two Panasonic Lithium Ion NCR 18650 batteries, with nominal voltage of 3.7 Volt and nominal capacity of 3.3 Ah in parallel configuration. The

criteria for their choice are their small weight and compact dimensions, compared to other batteries of the same nominal voltage and capacity.

The SLAVE circuit is powered by two HLR 1223W lead batteries with nominal voltage of 12 Volt and capacity of 5 Ah in parallel connection. The criteria for choosing them are that, unlike other lead batteries, they do not produce gases during charging/discharging so they can be hosted in a sealed housing as the one of the ASP. Their disadvantages comparing to lithium batteries are their larger weight and dimensions.

2.3.8 ASP navigation

The ASP navigation module is based on a high accuracy pressure sensor that controls the vertical movements and navigates the system by triggering the VBS mechanism. The ASP pressure sensor is a PA-21D KELLER that meets the operational needs of the system and can be embedded to control circuit. The outer housing of the sensor is made of high-strength stainless steel. The electronic circuits inside the sensor are covered by a glass casing filled with oil, which protects them from external pressure and electric field interference. The PA-21D KELLER specifications are:

Dimensions	11mm × 4.2mm
Range	1 ... 30 bar
Accuracy	± 0.15% FS
Total error band	± 0.5% FS
Operating temperature	-40 ... 110 °C
Response time	<4 ms
Input	1.8- 3.6 VDC
Power Consumption (active mode)	1.5 mA
Power Consumption (sleep mode)	100 nA

The pressure sensor calibration is performed using equipment of the sensor manufacturer following the appropriate guidelines. An electronic calibration gauge is used as a valid source of pressure measurement, which, compared to the pressure gauge, gives an insight into the accuracy of its measurements. The manually operated pressure oil pump (0 to 700 bar) was used to simulate different pressure environments in the pressure sensor. It has an oil filler tank and two special receptacles where the pressure sensor is mounted on one and the electronic pressure gauge on the other. The pump has the ability to apply the same pressure to both receptacles, resulting in the pressure values measured by the sensor and the manometer being compared with reliable results (Figure 7).



Figure 7: The ASP pressure sensor calibration procedure

The calibration experiment results revealed that under constant pressure conditions the maximum error of the pressure sensor is +0.13 (bar), while in conditions where the pressure is varied its maximum error is +0.03 (bar) (Figure 8).

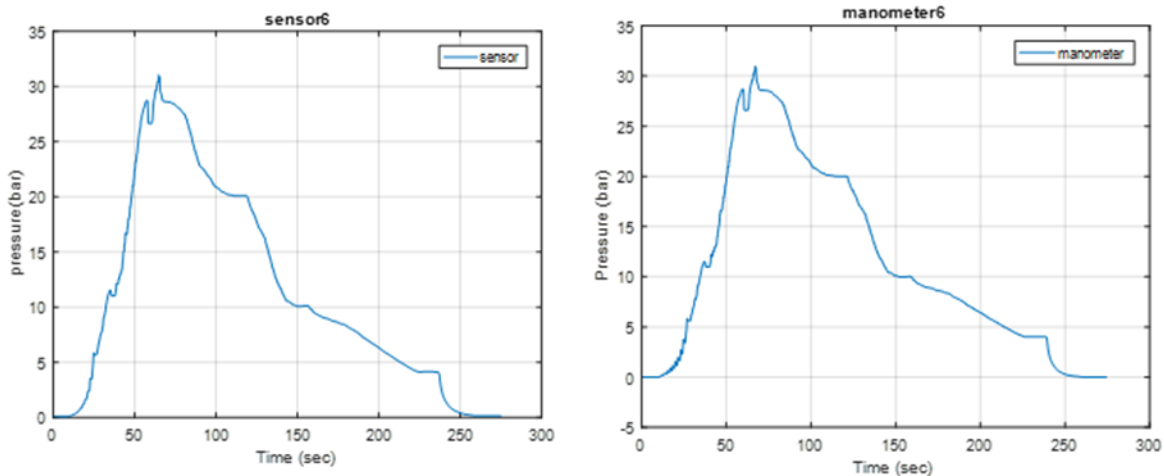


Figure 8: The ASP pressure sensor calibration diagrams (left panel: the ASP pressure sensor reading, right panel: the calibration manometer readings)

2.4 ASP housing and variable buoyancy laboratory testing

2.4.1 Housing testing

The ASP housing was connected with a vacuum pump and the internal of the housing was under pressured to 0.2 Bar and remained sealed for 60 minutes. During the experiment the internal pressure

was steady (Figure 9) proving that the ASP housing is sealed from the external environment and can be deployed at the field.



Figure 9: The ASP housing internal pressure test

2.4.2 VBS testing

The second laboratory test was performed to establish the correct operation of the electronic and hydraulic circuits. A magnetic switch was added to the electronic circuit in order to power on the system without removing the housing. The manual hydraulic pump was connected to the pressure sensor and it was used to simulate the deployment depth of 50 meters. The ASP responded successfully performing a full cycle of descent/ascent procedure by moving the appropriate amount of oil from the external bladder to the internal and vice versa.

2.5 ASP housing and variable buoyancy field testing

The first field testing of the ASP was performed next to HCMR facilities in Gournes and the ASP was deployed attached to small mooring line in depth of 15 meters (Figure 10).

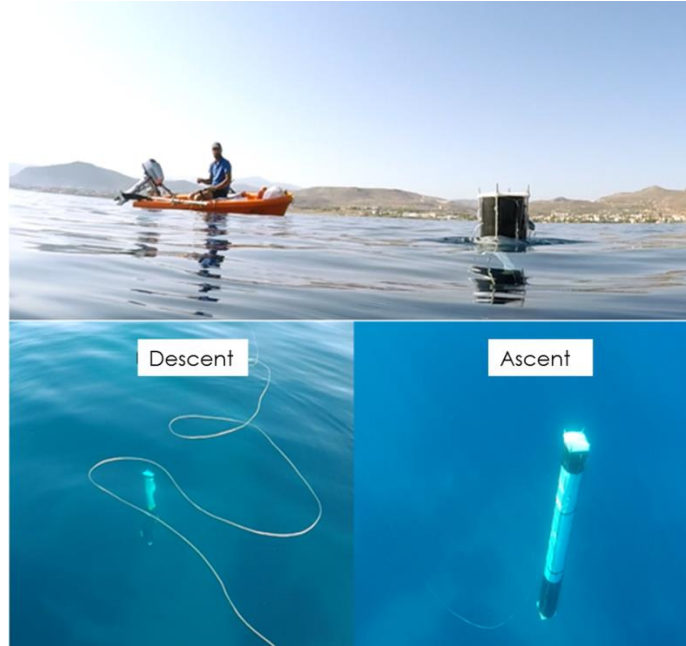


Figure 10: The ASP descending /ascending during the first field trials

The objective of the tests was to be able to study the descent/accnt speed in realistic environment and proceed with the final tuning of the variable buoyancy mechanism. The test results are presented in Figure 11

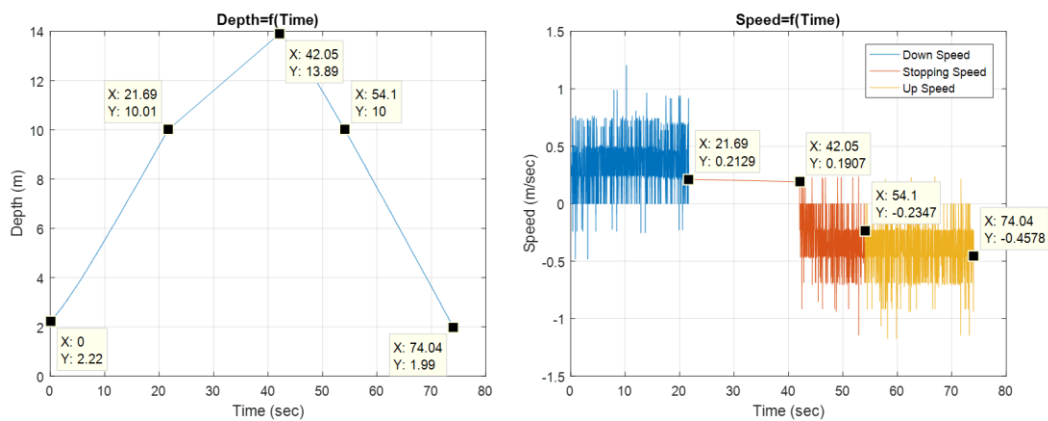


Figure 11: Left panel the ASP pressure sensor (depth) reading, right panel the ASP speed readings during ascent/descent

3 Autonomous underwater vehicle

3.1 Introduction

Fish-cage dysfunctionalities in aquaculture installations can trigger significant negative consequences in the operational costs. Fish escapes (through net holes) or decreased growth performance and /or feed efficiency (as a result of low oxygen levels due to excessive fouling) are just a few of the most common reasons. Therefore, frequent periodic inspection of fish-cage nets is required, but this can be a very expensive task. Small sized, low-cost autonomous devices can offer a lower cost alternative solution, providing also more frequent inspections and efficient timely alarming. As there is a trend to move aquaculture installation sites away from shore (to avoid competition, to increase farming sites, to reach more appropriate environmental conditions), it is important to achieve the complete operational and energy autonomy and frequent status reporting.

Within TAPAS, HCMR has developed and demonstrated a small-sized Autonomous Underwater Vehicle (AUV) that can be used for regular periodic fish-cage net inspection. The AUV system uses advanced optical recognition techniques to automatically detect fish-cage nets integrity problems and connects to communication networks to alert the designated personnel upon problem detection. In addition, using a docking-station it can automatically recharge its batteries so that its operation remains unhindered. In this way, appropriate corrective measures may be taken to avoid or minimize escapes and the related maintenance and repair costs.

The proposed AUV can be permanently reside in fish-cages and provide near-real-time information about the net integrity and the general cage status. To improve the system's efficiency incorporation of additional sensors and measurement devices aboard are into consideration for the next version e.g. biomass estimation, feeding efficiency monitoring etc.. The AUV will be initially configured to perform a single net inspection daily, so as to leave plenty of time for battery charging, data uploading and other maintenance routines. Current battery capacity allows for additional missions during the day if it is necessary.

3.2 Monitoring concept and System Description

The AUV monitoring system comprises of the following subsystems:

- The vehicle (AUV)
 - Vehicle and Sensors
 - Inertia and Optical Navigation System (on board real time optical processing)
 - Data Storage and Communication
- Off-line processing and Communications
 - Storage
 - Image Processing (off-line optical processing for net dysfunctionalities detection)
 - Communications / Alarming
- Energy Provision and management
 - Charging Docking Station

3.2.1 AUV – Vehicle and Sensors

The AUV is based on the commercially available Bluerobotics BlueROV2 Platform (Figure 12) [2] which has the following characteristics: 6 thrusters in a vectored configuration, Internet connectivity, Raspberry companion computer, PX4 autopilot module, 3D acceleration sensors, depth-meter and 3D magnetic compass, 1080p camera, swappable LiPo battery and 100m depth rating.



Figure 12: ROV platform

3.2.2 Conversion of the ROV to AUV

The Remotely Operated Vehicle (ROV) was converted to an AUV by incorporating additional s/w and h/w subsystems that make possible the autonomous movement taking care of the challenges that are associated with the autonomous operation of a submersible device:

- the location and navigation of the vehicle, (as GPS is not available underwater) using a combination of inertia and magnetic sensors with real-time machine vision algorithms
- communication data-rates, as microwave wireless communications are not possible underwater
- battery recharging, using inductive charging techniques

To increase the communication speeds with the land base, the AUV is programmed to dock to a near-surface-based docking-station that has a direct link to the internet. Through this link, the time-tagged and position-tagged HD video can be uploaded to a land-based server for further image processing and fish-cage net integrity inspection.

The docking station is also used for the inductive charging of the AUV batteries. Special optical recognition navigation is engaged to direct the AUV in the appropriate position when the daily mission ends, or when battery energy levels fall below a predetermined level.

The AUV is programmed to perform a predetermined course in the cage, in order to record video of the total fish-cage net area. During its mission, it stores the video in an on-board storage memory. Upon mission completion, the AUV is automatically guided to the docking station for data uploading and battery charging.

3.2.3 Optical Navigation

The AUV is programmed to perform a predetermined course in the cage, in order to record video and scan the total fish-cage net area, saving the video in an on-board storage memory. For the acquisition of underwater image data and the automated inspection, a methodology to efficiently navigate the AUV equipment under real operational conditions is required. The navigation procedures are performed without a user, based on information (positioning and distance) extracted from automated recognition of reference targets via processing optical data captured by the AUV camera. Towards this, a simple (to ensure efficient CPU power usage) yet accurate and robust approach is needed, enabling real-time processing and assessments. The proposed navigation scheme is based on an optical recognition/validation system combined with photogrammetry fundamentals applied to a reference target of known characteristics attached to the net.

In order to address the fish net consistency inspection problem, video data from successive monitoring of the entire fish-cage area under a relative close distance (from the surface till the bottom of the cage) need to be collected. This procedure is illustrated in Figure 13 and achieved via the following scheme:

Given a target attached to the net (black square with white-colored borders), navigate the AUV to detect the object under a certain distance from it and scan the net via a polygonal route to detect abnormalities under the following algorithmic steps [3]:

1. Rotate and sink the AUV to meet the compass and depth sensor known spot of the reference target (the target attached to the net is located at known compass heading and depth, thus the AUV turns towards the expected direction and position with respect to the surface in order to start searching)
2. Move the AUV till the target is detected (successive detection within a time interval so as to ensure valid detection and avoid outliers)
3. Translate the measurements from image space to real world (machine vision process) under the appropriate mathematical model
4. Export desired parameters (target coordinates within the image, target id, distance from target) to the AUV navigation routine
5. Move the AUV to forward/backward direction to meet the desired distance from the target
6. Perform the net monitoring following a perfect polygonal route, correct contour if required (divergence operational distance from the net is detected)
7. Detect the next reference target and correct movement if divergence from the designed route is detected
8. Complete a full fish-cage "route", dive to the next depth level and repeat procedure

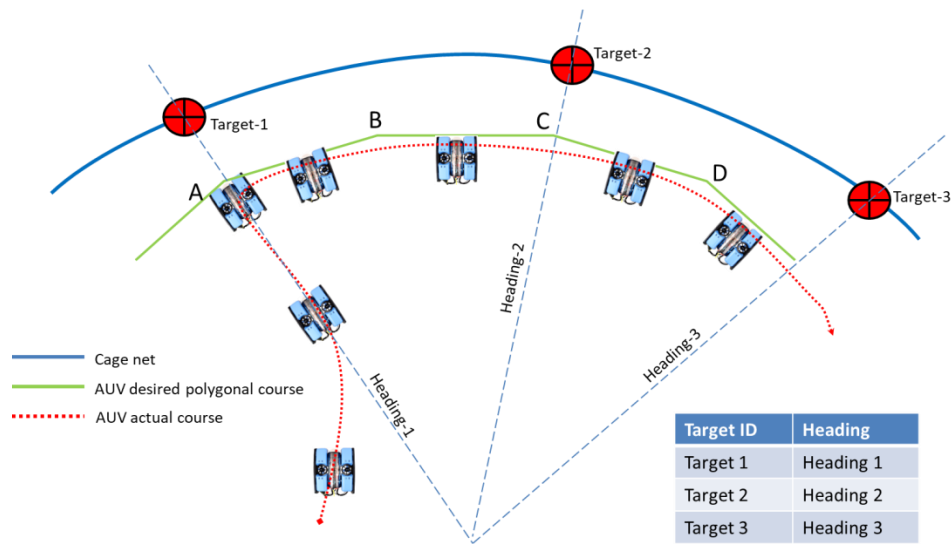


Figure 13: AUV Optical Navigation using targets

In order to further enhance the navigation approach, we introduce the “texture-index” [4] and associate it with a preliminary yet indicative evaluation of the distance from the net. This index can be considered as a metric to determine the presence of high-textured objects [5], i.e. structures constituting of repetitive patterns, such as the fish-cage-net in our case. High values of this metric indicate that the AUV approaches closely to the net, while small ones reveal that the AUV draws away from the net. This is very important to the fish-cage net inspection procedure, since potential risks, deadlocks and damages along with divergence from desired route, due to net deformation caused by water currents, or vehicle malfunction can be anticipated [6], [7], [8].

In addition, by examining the difference of the index values in the left and right parts of each frame, we can estimate the angle between the net surface and the AUV’s longitude, and provide appropriate control commands to keep it reasonably close to the ideal value of 90°.

The course navigation algorithms are executed on an additional on-board computer (ODROID XU4, octal-core, 2GB RAM, 64GB storage) [9] which appropriately combines the data it receives from the on-board sensors (depth-meter, magnetic compass, gyroscopes and accelerometers) and the output of real time target recognition processing.

3.2.4 Optical Net Inspection s/w

The main purpose of this work is to provide a tool for an automated mechanism for early detection of holes on the net (Figure 14) that will help with decision making on whether to take immediate action and fix the problem (hole patch) or leave it as is (small hole) until the next planned diver actions.

The scope of the software is the detection of potential problems that may arise in the underwater infrastructure (fish net), like holes, “broken” patterned structure, etc. Advanced image processing techniques (image feature analysis, texture analysis, pattern matching, closed curve analysis) are used for the calculation of all parameters that accurately describe discontinuities in the net structure.

Preliminary regularity analysis for patterned texture inspection has been performed resulting in a robust methodology capable of outlining the defective region in the underwater net images.

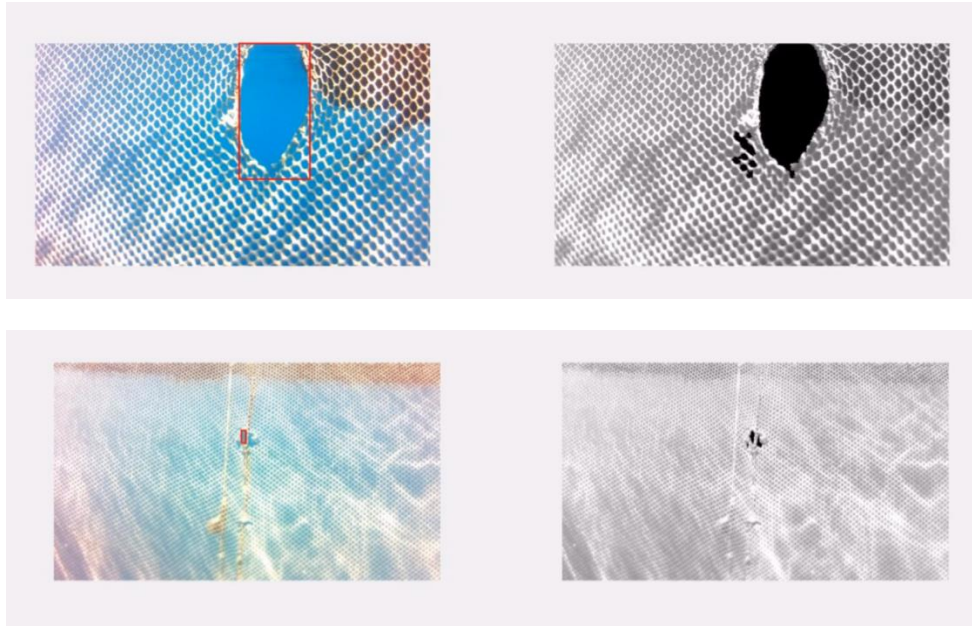


Figure 14: Cage net inspection s/w screenshot

The Optical Net Inspection software uses as input the video recorded during the AUV's mission from its on-board camera, and inspects it off-line using machine vision algorithms, to identify and report holes of various shapes and sizes.

In general, advanced image processing techniques like image analysis features, texture analysis, pattern matching, closed curve analysis etc. can be used for the calculation of all parameters that accurately describe discontinuities on the net structure. A first set of parameters that describe the existence of problems on the net can be derived using either the colour characteristics of the images or the net pattern [4], [10]. To begin with the appropriate methodology design and having in mind that it must be robust in order to be able to outline the defective region in the underwater net images, we first studied the net consistency in order to find discontinuities on the net pattern. As input, we used underwater net images captured under different illumination and zoom factor conditions and we studied the regularity feature for finding common properties in the patterned texture of the net. In general, regularity analysis (periodicity) of patterned textures involves two issues: the spatial relationship between intensity values or the repeat distance of a repetitive unit. As a first approach, we implemented cross correlation techniques that provide a correlation between the entire underwater image and the single net hole structure (or a small group of them). The main idea of the method is that all possible shifts of the template image are analyzed, in both positive and negative direction, meaning at every pixel of each image. As a result, it provides a measure for how well the template image fits with each shift. The proposed method is a kind of template matching and it is able to identify defects with differential pixel intensity changes like in the case of broken net pattern structure.

3.2.5 Docking-station

In order to achieve full autonomy and eliminate any cable connecting the AUV with the land-based world, an appropriate docking-station is used. It is equipped with inductive (wireless) charging hardware, enabling AUV battery charging when the latter is “docked”, and a wireless communication module, that allows data uploading after mission’s end. The docking station is powered through a Power-Over-Ethernet connection that provides also connectivity to the Internet and the corporate data network.

The wireless charging system has been designed and implemented in Printed Circuit Board (Figure 15).

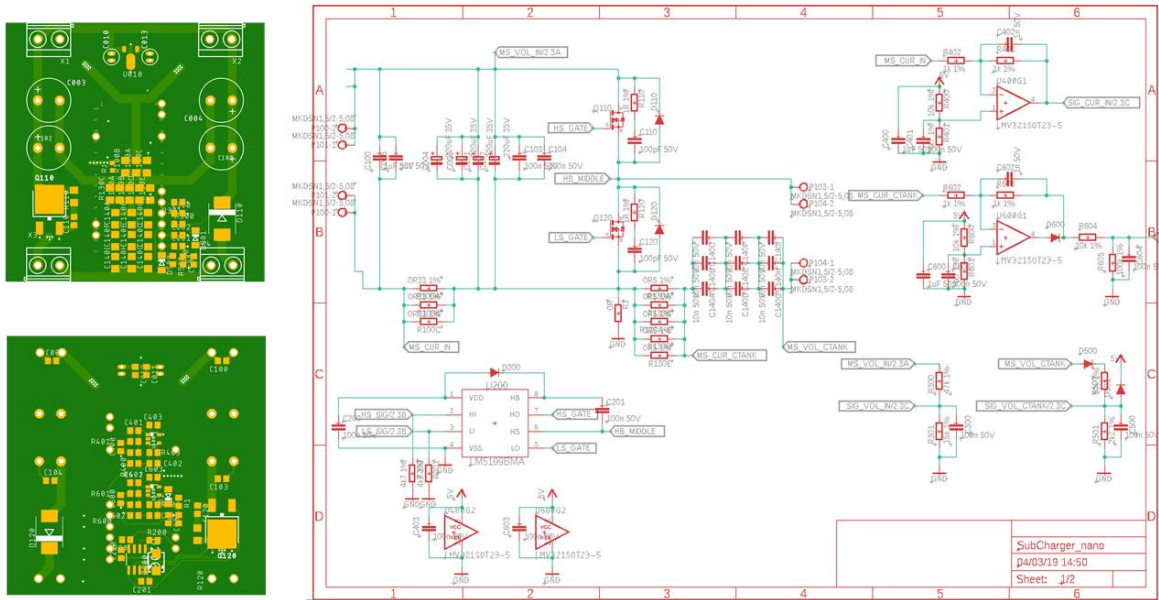


Figure 15: PCB (top and bottom side) and Schematic Design of the Wireless Charging Circuit

Two such circuits have been assembled following the “Master-Slave” approach, the first located on the docking station, and the second aboard the AUV, inside an additional submergible housing.

Using the electromagnetic inductance properties of two appropriately placed coils (both on the AUV and the docking station), the circuits will sense the successful docking of AUV in the docking station and will enable wireless battery charging and data exchange.

3.2.6 Implementation of the wireless Charging system

The two boards of the wireless charging system were implemented (Figure 16) and tested in the laboratory environment. The initial testing results are promising, since the system can wirelessly transfer approximately half of the energy it receives in its input. This means that it is possible to transfer a charging current of approximately 1 Amp/12V DC, using a source of 25Watts (24VDC). This power can also adequately power the AUV during the data transfer procedure.

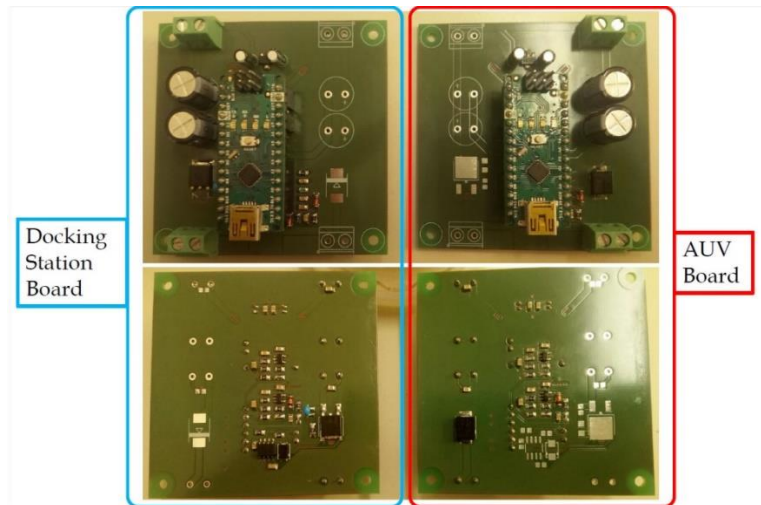


Figure 16: Wireless Charging System boards

The system was tested on the lab bench in order to measure its performance and energy transfer efficiency. The first tests (Figure 17) indicated that the system requires a relatively precise alignment that will also remain stable during operation. The same tests indicated that the optimal distance between the coils, achieving ~50% efficiency is 1-2 cm. At those figures, we can presume that the water layer's thickness will be almost negligible, because the thickness of the coil enclosures will ensure the correct positioning in the vertical axis.

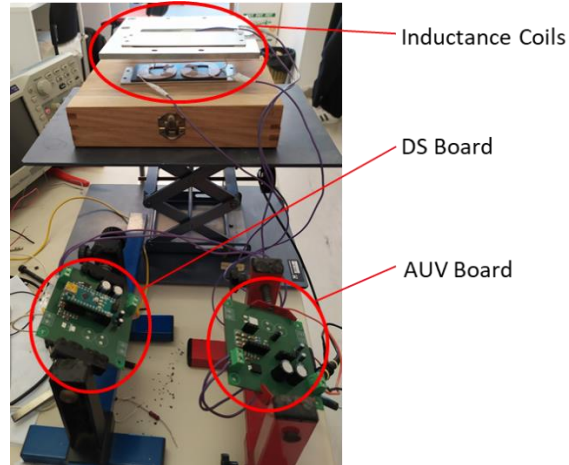


Figure 17: Wireless Charging System - Lab Test Environment

The effect of water currents on the docking accuracy, and the precision of the relative charging coils alignment, plays a dominant role in the efficient power that can be transmitted through the inductive charging system to the batteries.

3.2.7 Docking procedure software implementation

The Navigation System detects a particular “docking station target”, (Figure 18) that will be placed directly under the docking station. The detection of this target allows a relatively precise

vertical/horizontal positioning of the AUV with respect to the docking platform ($\pm 10\text{cm}$). At the end of this procedure, the AUV will be parked in a position that enables battery charging and wireless data exchange. During the docking, battery charging and data uploading are performed and upon successful termination the AUV enters to a state of “readiness”.



Figure 18: Docking Station Target (AUV Camera view)

The software with the aforementioned functionality has been integrated within the Navigation system and a number of tests were conducted in controlled environment. During these tests, the underwater transmission of Wi-Fi signals was also assessed. It is well known that 2.4 GHz signals’ attenuation in the water is quite strong [11], but we measured achievable transmission rates of 10Mbps in distances of $\sim 10\text{cm}$. This distance is larger than the optimally required 1-2 cm between the charging coils, and therefore this is not considered a problem in the specific application.

3.3 Trials of the AUV System in the fish-cage test facility

A squared fish-cage ($6\text{m} \times 6\text{m} \times 8\text{m}$) was used for test and trial in real conditions. Twenty-four optical targets were placed in several pre-determined positions in order to be used for the AUV Optical Navigation s/w during the net inspection missions (Figure 19).

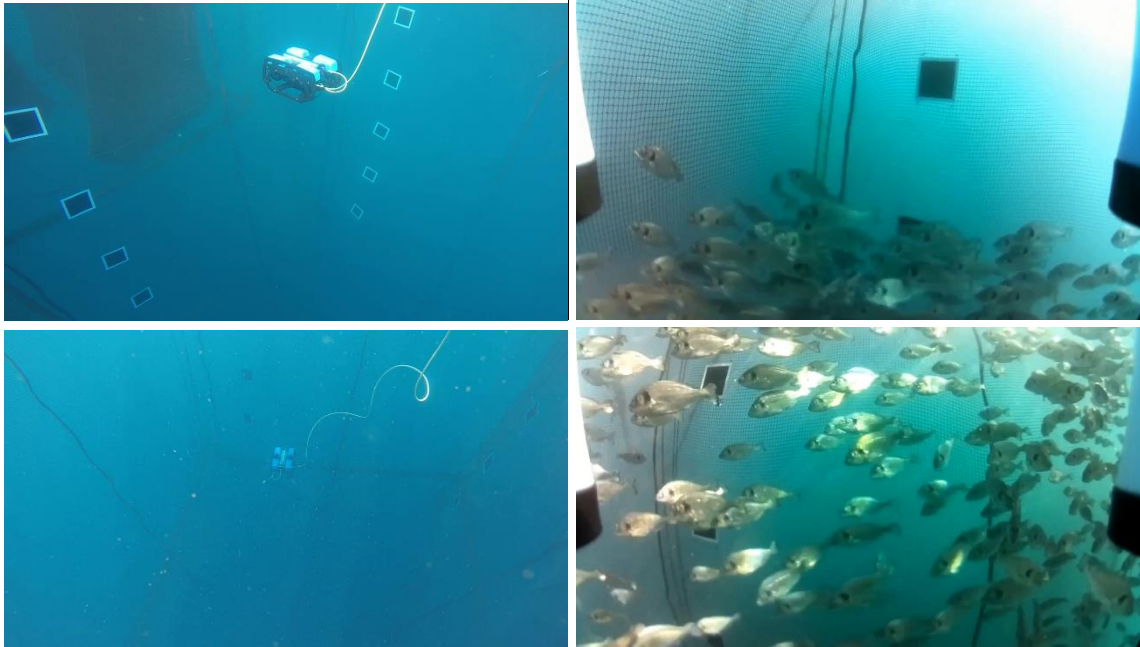


Figure 19: AUV Trials in fish-cages

Test-missions and trials were conducted in various lighting conditions and depths, with and without fishes in the cages and under different conditions. The most important conclusions of the testing process were the following:

- Selecting the appropriate operating AUV cruising speed is complex, as it depends on the strength and direction of water currents during the mission execution. In general, constant and low AUV speeds relative to the net are preferable. When strong water currents are present, maintaining nearly constant cruising speeds, while moving sideways scanning the net, is not feasible without additional hardware (range finders and/or more processing power) aboard
- When stocking density is low ($< 5\text{kg/m}^3$), fishes interfere only marginally to the navigation process and video recording of the total net's surface is possible



- When the stocking density increases ($> 5\text{kg/m}^3$) fishes interfere severely to the video recording of the net making it difficult or impossible to obtain a full scanning of the net's surface. To overcome this problem it is necessary to achieve smaller distance from the net, requiring additional processing power and/or range-finding hardware



- Operating in depths up to 10m does not require additional lighting, even with the low-cost, low-sensitivity camera currently used
- Vertically frequent positioning of targets (~80cm center-to-center distance) facilitates the consistency in high target recognition rates and simplifies the scanning mission's configuration
- Using the "Texture Index" metrics to maintain a proper viewing angle of the net proved to be efficient, as the AUV automatically adjusts its course and follows the net's shape

The overall conclusion of the trials can be summarized in that the optical navigation of the AUV inside a fish cage and the automatic reporting of inspection results are feasible at lower stocking densities. Additional means (range finders and more processing power) are necessary when stocking densities increase towards industrial norms.



4 Autonomous above water radiometer system WISPstation

4.1 Monitoring concept

Water quality remote sensing techniques are based on the concept that the concentrations of optically active water constituents determine the exact colour of the surface water. Detailed observations of the water colour can thus be used to derive these concentrations. Water Insight follows the protocol for obtaining the subsurface reflectance as published by Gons [20], consisting of sets of up- and downwelling radiance and irradiance measurements. The optimal angles for observation are identified by Mobley [12] and his measurement geometry is discussed below.

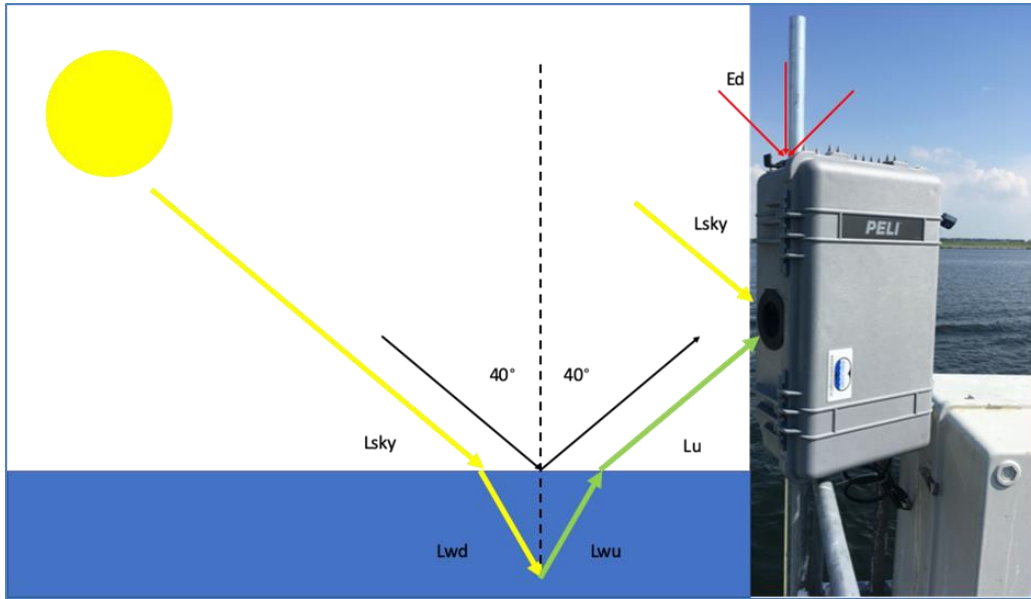


Figure 20: WISP Station concept

In order to reduce the chance of direct reflections of sunlight from the water surface (sun glint) radiance measurements should be taken in a direction of 135° out of the plane of the sun. To avoid using a rotating platform (as moving parts are unwanted in the design) the WISPstation is equipped with a double setup of radiance sensors so at any time at least one sensor is looking away from the sun (Figure 20).

The steps leading from reflectance measurements to the retrieval of water quality constituent concentrations is given in the next section, starting with an overview of parameters included in Table 1.

Table 1: Overview of parameters used in optical water remote sensing

Parameter	Unit	Description
Rrs	$[\text{sr}^{-1}]$	Above water radiance reflectance or (above water) remote sensing reflectance
rrs	$[\text{sr}^{-1}]$	Under water radiance reflectance or under water remote sensing reflectance
R(0+)	[-]	Above water irradiance reflectance

$R_{(0-)}$	[-]	Irradiance reflectance just below the water surface
ρ_w or R_w	[-]	Water leaving reflectance which is a irradiance reflectance = $\pi * r_{rs}$
L_{up}	$W m^{-2} nm^{-1} sr^{-1}$	Above water measured upwelling radiance (water leaving radiance + reflected sun and sky radiance)
L_{sky}	$W m^{-2} nm^{-1} sr^{-1}$	Above water measured downwelling radiance (sky radiance)
E_d	$W m^{-2} nm^{-1}$	Above water measured downwelling irradiance (sum of direct and diffuse irradiance)
ρ	[-]	Conversion factor (or spectrum) to calculate the part of the sky radiance that is reflected by the water surface into the Lup sensor
n	[-]	Refraction index from air to water ($n = 1.341$ for ocean waters and $n= 1.333$ for freshwater)
r^0	[-]	Fresnel coefficient for 0 degree angle of incidence ($r^0=0.021$)
f	[-]	Pre-factor by Walker (1994)
a	m^{-1}	Total absorption
b_b	m^{-1}	Total backscattering

The WISPstation takes two sets of measurements for each cycle (one for each set of sensors). After proper calibration and quality control there is a preferred measurement set containing the upwelling radiance L_{up} , the downwelling sky radiance L_{sky} and the downwelling irradiance E_d . First the above water Remote sensing reflectance (R_{rs}) is calculated according to:

$$R_{rs} = \frac{L_{up} - \rho L_{sky}}{E_d} [sr^{-1}]$$

There are several ways to calculate ρ :

1. Fixed value: this is done for the WISP: $\rho = 0.028$ [12]
2. ρ is still one number but determined from the noise in R_{rs} ([23])
3. ρ is a spectrum determined with the 3C model [13]

WISPcloud uses the R_{rs} with a fixed ρ for the moment.

In order to link the reflectance measured above water with the WISPstation to the reflectance modelled from the water constituents we need to recalculate R_{rs} to the below water remote sensing reflectance $R_{(0-)}$:

$$R_{(0-)} = \pi * 1,80 * R_{rs} [sr^{-1}]$$

Now, the presence and abundance of optically active natural water constituents is revealed by recording the colour of a water body by remote sensing instruments. The water colour spectrum is an apparent optical property (AOP) of the water. Its value changes with the optical properties and concentrations of the optically active substances in the water (the inherent optical properties or IOPs). In the field of water remote sensing the relationships between the concentrations of the mentioned water quality parameters and the resulting water colour are studied by means of bio-optical models. Correct calibration of these relationships/models is a prerequisite for successful inversion and the determination

of concentrations of water quality parameters from observed spectral remote sensing data. Using the Gordon-Walker model the AOPs absorption and backscattering can also be used to model the $R_{(0-)}$:

$$R_{(0-)} = f \frac{b_b}{a + b_b} [sr^{-1}]$$

In the case of WISPcloud, we use robust and published semi-empirical band ratio algorithms to retrieve water quality parameters from the reflectance signal.

These band ratio algorithms are:

- Chlorophyll-a concentration (based on Gons [20])
- Total suspended matter (or suspended particulate matter) concentration (based on Rijkeboer [21])
- Vertical diffuse attenuation coefficient (based on Gons [19])
- C-phyococyanin concentration (based on Simis [22])

4.2 System description

Originally off-the-shelf commercially available autonomous above water radiometers would be used within TAPAS. However, at the project start the company that offered those, BlueLeg Monitor, ceased all its activities. It was therefore decided that WI would in turn develop its own radiometer system within the project by switching most of the budgeted equipment costs to personnel costs. This development led to the WISPstation. The WISPstation records radiance and irradiance with an extended wavelength range of 350 to 1100 nm in two viewing directions, which enables continuous and autonomous high-quality measurements for water quality monitoring and satellite validation. All channels are measured with a single spectrometer and an optical multiplexer. This design makes resulting remote sensing reflectances, less sensitive to radiometric and spectral calibration errors and drifts. In various Copernicus projects (TAPAS, EOMORES and MONOCLE) the WISPstation is being tested in highly diverse water types and environmental conditions, ranging from case-1 in Mediterranean coastal waters to turbid waters with cyanobacteria proliferation in lakes and lagoons. In view of its initial scientific application, the system is designed to reliably produce high frequency observations to quantify variability in physical and biological water system parameters. The WISPstation results are stored in the online database WISPcloud allowing users to extract data for analysis. A web interface is being set up to visualise the measurements. We present spectral results and time series analysis for various locations.

Several essentially different viewing geometry designs for above water optical systems have been proposed in literature such as:

- a) The sun-following design with one-radiometer (Seaprism, [14], or with 3 radiometers, (Dalec, [15])
- b) The one viewing angle 2 radiometers system with the L_{up} sensor under water [16]
- c) The two (or more) fixed viewing angles system [17]

Basis for designs a) and c) are the considerations by (Mobley, 1999, [12]), namely azimuth angle is optimal around 138 degrees from the sun, L_{up} angle is around 42 degrees from the nadir and L_{sky} angle is

around 42 degrees from the zenith. With varying geometry, Mobley proposes a table of coefficients to account for surface reflections at various wind speeds and solar position.

Table 2: Different instruments used for the data analysis in this report and the various instrument specifications

Instrument	TriOS Ramses	WISPstation	WISP-3
Wavelength range	320-950nm	350-900nm	400-800nm
Field-Of-View for radiance sensors	7°	1.3°	2.8°
Viewing angle (from nadir)	41°	40°	42°
Viewing azimuth angle	‘East’ sensor: 135° (SE) ‘West’ sensor: 225° (SW)	Starboard sensor: 157.5° Port sensor: 202.5°	‘Wrong’ direction: ~180° ‘Correct’ direction: 45° left/right of sunlight direction
Integration time	4 ms – 8 sec (for both irradiance and radiance)	Maximum 4 sec (no measurement stored)	Depends on light conditions ¹
Full width at half maximum (nm)	~12	4.65	4.9

The WISPstation is based on a modification of the Wernand design using two sets of sensors looking NNW and NNE instead of NW and NE. It should preferably be installed looking in a northward direction (on the Northern hemisphere) providing two optimal viewing geometry moments during the day and a large time window with acceptable viewing geometries that can be accounted for. The advantage of a fixed system with two viewing directions is that there are no moving parts, robots etc. which makes the system less costly, better to maintain and less prone to malfunctions.

In total the WISPstation features 8 channels:

- 2 Radiance channels collecting L_{up} and L_{sky} in the NNW direction
- 2 Radiance channels collecting L_{up} and L_{sky} in the NNE direction
- 2 Irradiance channels
- 1 unexposed dark radiance channel for evaluation of radiance channel degradation
- 1 unexposed dark irradiance channel for evaluation of the degradation of irradiance channels

All channels are connected to the central spectrometer by means of optical fibres and an optical multiplexer. The advantage of this design is, amongst others, that any variability or degradation of the sensitivity of the spectrometer is compensated in the calculation of remote sensing reflectance. A regular measurement cycle where each channel is measured 10 times at an optimal integration time takes usually less than 1 minute depending on ambient light conditions. The system is calibrated relative to a reference instrument. The reference instrument is calibrated in a certified laboratory using a lamp and integrating sphere with NIST traceable calibrations.

¹ During the field campaign, integration time was sometimes found to take more than 4 seconds (WISP3 screen will show ‘Acquiring light...’), with no particular relationship with the amount of light. Instrument specifications were supplied by Water Insight and also taken from Hommersom et al. (2009) [18] and Tveiterås (2013).



The WISPstation is watertight and built into a highly climate resistant case. Temperature of the sensor and humidity in the case is registered along with every measurement. Data are transmitted to the database (“WISPcloud”) autonomously through a cellular connection. The instrument can be remotely accessed and e.g. updated or configured to a specific time interval or measurement frequency. It is autonomously powered by a solar panel and internal large battery.

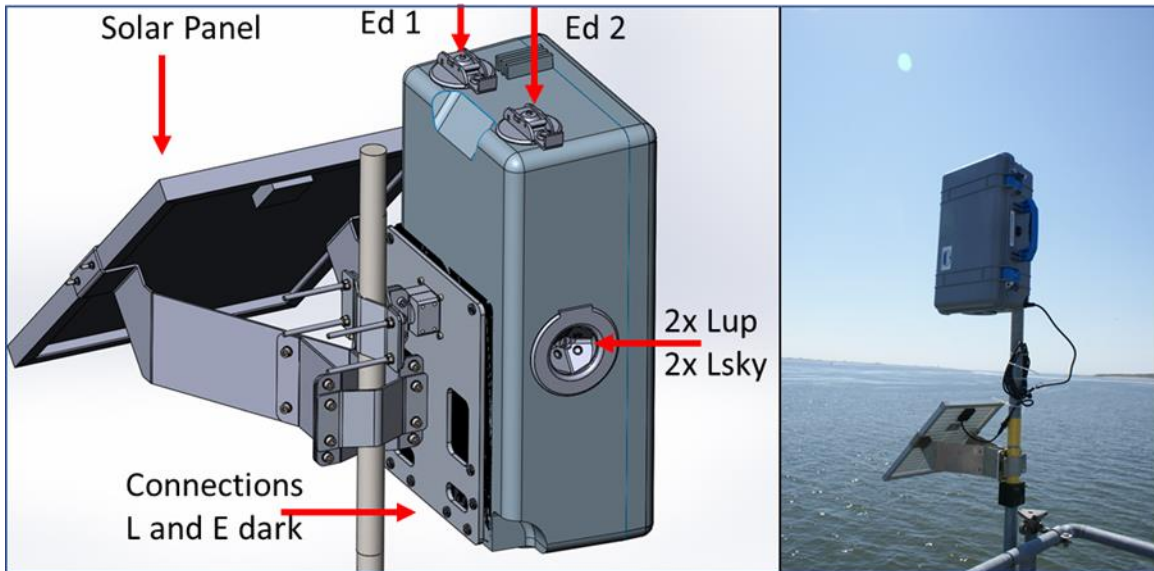


Figure 21: Layout and installation of a WISPstation

Currently the WISPstation is built around the Avantes Mini mk-1 spectrometer with a maximum wavelength range between 220 and 1100 nm. The grating has 300 lines per mm with a blaze of 300 nm. Together with a slit of 100 μm this leads to a spectral resolution (FWHM) of 4.65 nm. Stray light is reported to be lower than 0.2%. The WISPstation spectral characteristics are to some extent configurable. The Avantes Mini is a rugged spectrometer designed for use outside of laboratories. Serial production by assembly robots warranty very small differences between instruments. While the standard measurement frequency is set to once per 15 minutes, it can be increased to once per two minutes if required, e.g. in intervals around satellite overpasses.

The most important characteristics are summarized in Table 3.

Table 3: Specifications of the WISPstation

Specifications of the WISPstation:	
Wavelength range :	Max: 220-1100 nm (depends on calibration)
Channels	
5 Radiance channels:	2 * L_{up} and 2 * L_{sky} (both sensor sets look at opposite angles away from the sun):
3 Irradiance channels:	2 * upward looking
Unexposed reference dark channels:	1 * radiance and 1* irradiance

Physical characteristics	
Grating: Lines per mm: 300	Blaze (nm): 300
Slit: 100 μm	FWHM (at 100 μm slit, 300 lines / mm): 4.65 nm
Stray light: <0.2%	Signal/Noise: Min 300:1
AD converter: 16 Bit 2MHz	Integration time: 1.05 ms to max 10 minutes
Temperature range: 0-55C	Powering: Independent: solar panel
Internet Connectivity: 2 Way over 3G or WIFI	Pole size for attaching the instrument: 5 – 10 cm diameter
Measurements	
Measurement frequency: 1x per 15 minutes (adjustable)	Repetitions: Each channel is read out 10 times
Output: Quality controlled $R_{rs(0+)}$ at 1 nm	

4.2.1 Database and output API

A scalable Postgres database (WISPcloud) is available to autonomously receive and store all measurements, to perform quality control, to apply water quality algorithms and to serve data requests directly to customers through an advanced API. Work is in progress to provide access to the data through e.g. a Jupyter notebook. Internal quality control procedures are increasingly being put into place to identify and flag sub-optimal measurements.

Currently glint correction is handled in a basic way (fixed $\rho_{sky} = 0.028$), the results of research into advance options for glint correction (Groetsch et al., 2018) will be implemented soon.

For water quality monitoring purposes, the remote sensing reflectance observations are run through some standard water quality algorithms to make a first estimate of Chlorophyll-a (Gons, [20]), total suspended matter (Rijkeboer, [21]), Phycocyanin (Simis, [22]) and water transparency (Gons et al, [19]). For a short description of the API see TAPAS D7.2 Database for in situ measurements.

4.3 Operational deployment

4.3.1 Deployment at Souda Bay, Crete (Greece)

In collaboration with partner HCMR a WISPstation was deployed at the experimental fish farm in Souda Bay, Crete from 17-07-2018 until 30-08-2019. The fish farm is a relatively calm and clear water environment. The location and placement are shown in Figure 22 and Figure 23.

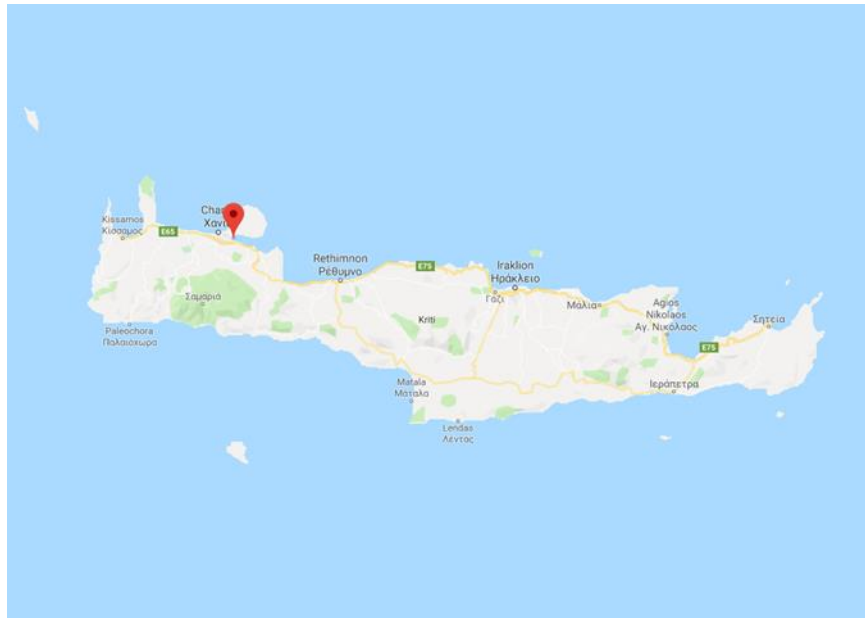


Figure 22: Location of the WISPstation at Souda Bay, Crete



Figure 23: Placement of the WISPstation

4.4 Example WISPstation results

Some examples of WISPstation reflectance spectra and time series plots are given in this section. Below some reflectance spectra collected on different days in Souda Bay are illustrated.

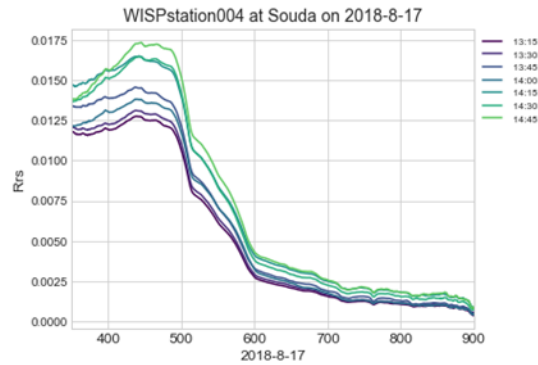


Figure 26: Example WISPstation R_{rs} spectra in perfect conditions

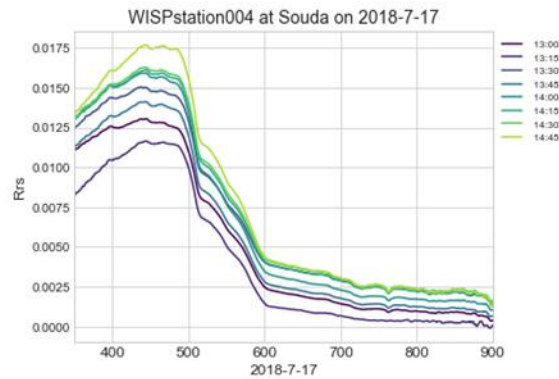


Figure 27: Example WISPstation R_{rs} spectra in slightly shaded conditions

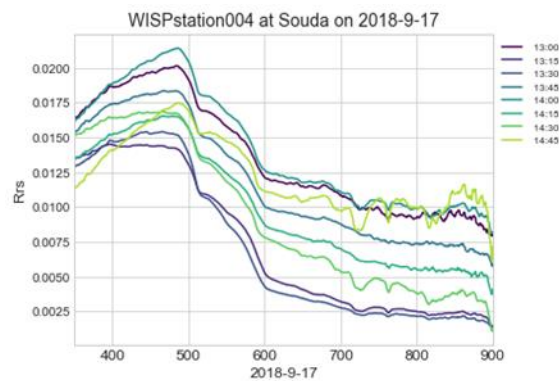


Figure 28: Example WISPstation R_{rs} spectra in bad weather

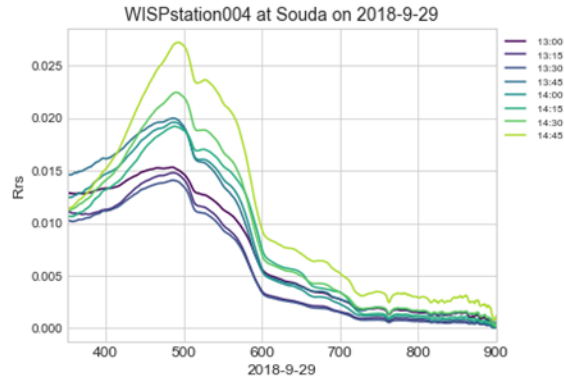


Figure 29: Example WISPstation R_{rs} spectra in showing effects of the storm on 29/9

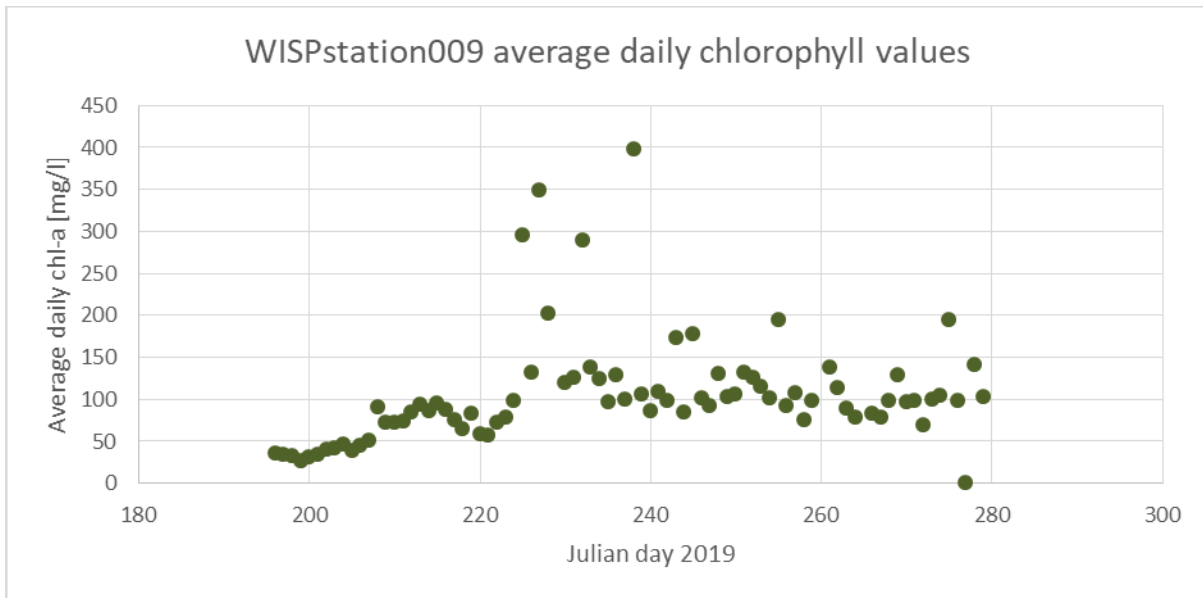


Figure 30: Chlorophyll-a measurements at the Hungarian station from 15-07-2019 until 08-10-2019

From concurrent studies it is known that the Chl-a algorithm produces reasonable results as the Gons family of algorithms is developed for inland turbid waters. The Chl-a values increase at the end of the summer and then stabilize (Figure 30). Another example is the time series of TSM of the Hungarian station (Figure 31), that also increases at the end of summer like Chl-a, but already starts to decrease in October.

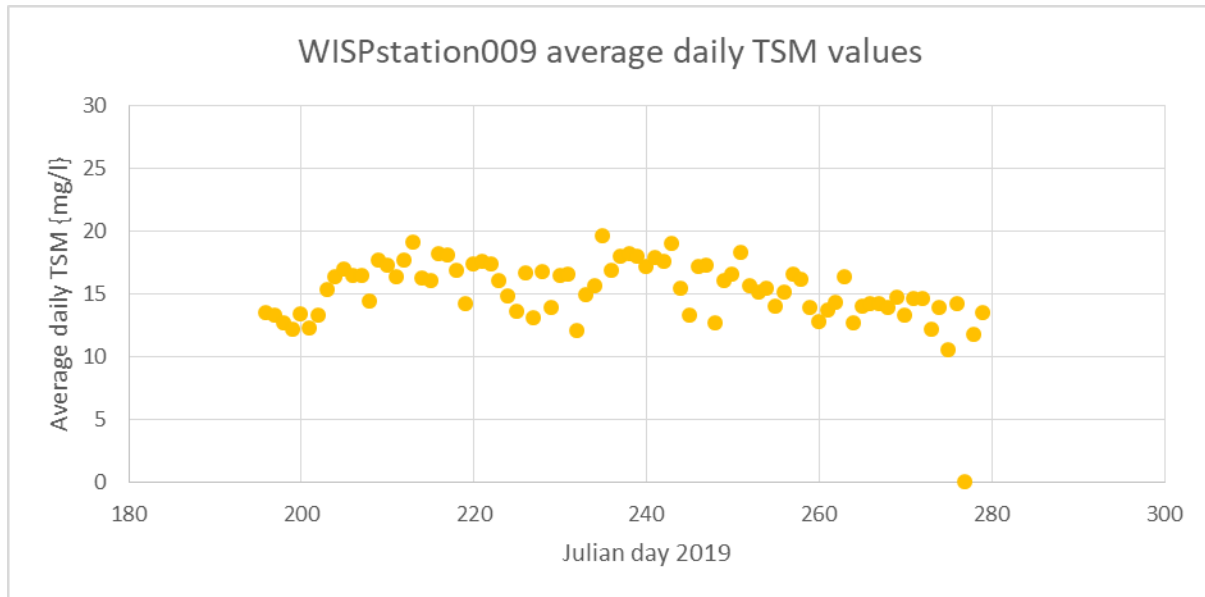


Figure 31: Sediment measurements at the Hungarian station from 15-07-2019 until 08-10-2019

The measurements for Souda Bay show little seasonal variation as can be expected from a Mediterranean coastal site.

4.5 System performance

For the WISPstation at Souda Bay, during the whole year of operation only minimal maintenance was required. Some outages occurred as a result of the power solution and some telecommunications problems. Minimal data was lost as the longest outage was 5 days. The power issues mainly happened in lasting cloudy conditions, preventing the solar panel that was less than optimal installed due to site restrictions to fully charge the WISPstation. Earlier in 2019 an update of the power solution has been developed and tested for the WISPstations to overcome this, but as the Souda Bay WISPstation was already deployed this upgrade is only due now it is returned. A total of about 15.000 quality-controlled measurements have been collected during the deployment. Most of the data will still be analysed in ongoing research.

The WISPstation at Halastó, Hungary has been running for three months in summer 2019. No significant outages have been reported during the deployment. This WISPstation has had the power system upgrade. Most of the data will still be analysed in ongoing research.

4.6 Link to TAPAS DST (recommendations for wider use)

The aim of TAPAS is to provide as much relevant information to the aquaculture sector as possible. High-frequency and high-quality monitoring using innovative in situ sensors are valuable in this highly regulated sector. Using the monitoring data from the WISPstation, but also from the PML spectrometer and the Autonomous Underwater Vehicle and from the water quality parameter maps derived from EO data, the TAPAS tools (incl. models) can be quantified, validated and improved.

5 Closing Remarks

In this report the results of Task 7.2 were presented in detail. The key objective of the task, as they were described in the TAPAS contract (“to deploy existing and develop new innovative systems for automatic in-situ measurements of physical, ecological and chemical water quality including novel biosensors and optical sensors as well as monitoring the integrity of the cage material”) was successfully achieved, with the development of:

- An Aquaculture Specific Profiler that carries out vertical profiles of the water from the surface to the bottom of the fish farm, with user configurable payload
- An Autonomous Underwater Vehicle that is able to perform regular inspections of the cage material condition and transmits alarms in case of problems detection
- An optical sensors based observation system providing ecological water quality measurements by recording radiance and irradiance and performs continuous and autonomous high-quality measurements for water quality monitoring and satellite validation

All three systems were successfully tested and demonstrated in their operational environment at selected test sites, reaching the TRL 7 (“System prototype demonstration in operational environment”).

Frequent and high-quality monitoring using innovative in situ sensors and systems are valuable in this highly regulated sector. Using the monitoring data from the three abovementioned tools, the TAPAS tools and models can be quantified, validated and improved. The work carried out in Task 7.2 and its results indicate that within the next few years, autonomous and intelligent systems may play a fundamental role in daily tasks performed in aquaculture installations, bringing a new era towards surveillance, inspection and intervention procedures. Following the current advances, new challenges and opportunities for commercial products applicable to the aquaculture industry will appear facilitating the routine operations and reducing the operational costs.



6 References

- [1] Martin Føre et al, "Precision fish farming: A new framework to improve production in aquaculture", <https://doi.org/10.1016/j.biosystemseng.2017.10.014>
- [2] Bluerobotics, Manual of the ROV, <http://docs.bluerobotics.com/brov2/>
- [3] G. Livanos, V. Chalkiadakis, M. Zervakis, K. Moirogiorgou, , G. Giakos, N. Papandroulakis 2018. Intelligent Navigation and Control of an Autonomous Underwater Vehicle Prototype for Automated Inspection of Aquaculture net pen cages. IEEE International Conference on Imaging Systems and Techniques, October 2018, <https://ieeexplore.ieee.org/document/8577180>
- [4] V. Chalkiadakis, N. Papandroulakis, G. Livanos, K. Moirogiorgou, G. Giakos, M. Zervakis 2017. Designing a Small-sized Autonomous Underwater Vehicle Architecture for Regular Periodic Fish-cage Net Inspection. IEEE International Conference on Imaging Systems and Techniques, October 2017, <https://ieeexplore.ieee.org/document/8261525>
- [5] Ms. Neha Shukla, Dr. Anurag Trivedi, "Image Based Distance Measurement Technique for Robot Vision using New LBPA approach", International Journal of Novel Research in Electrical and Mechanical Engineering, Vol. 2, Issue 1, pp: (22-35), 2015
- [6] Asgeir J. Sørensen, Martin Ludvigsen, "Towards Integrated Autonomous Underwater Operations ", IFAC-PapersOnLine 48-2 (2015) 107–118, 2015.
- [7] Budiyo, Agus, "Advances in unmanned underwater vehicles technologies: Modelling, control and guidance perspectives", Indian Journal of Marine Sciences, 38. 282-295, 2009.
- [8] Russell B. Wynn et al, " Autonomous Underwater Vehicles (AUVs): Their past, present and future contributions to the advancement of marine geoscience", Marine Geology 352 (2014) 451–468, 2015.
- [9] ODRROID XU4 technical description https://www.hardkernel.com/main/products/prdt_info.php
- [10] Martina Anelli et al, "Towards new applications of underwater photogrammetry for investigating coral reef morphology and habitat complexity in the Myeik Archipelago, Myanmar", Geocarto International, pp 1-23.,2017
- [11] Gwyn Griffiths, "Technology and Applications of Autonomous Underwater Vehicles ", CRC Press, ISBN 9780415301541 - CAT# TF1622, 2002.
- [12] C. D. Mobley, "Estimation of the remote-sensing reflectance from above-surface measurements," Appl. Opt. 38(36), 7442–7455 (1999), <http://dx.doi.org/10.1364/AO.38.007442.APOPAI0003-6935>
- [13] Groetsch, P.M.; Gege, P.; Simis, S.G.; Eleveld, M.A.; Peters, S.W. Validation of a spectral correction procedure for sun and sky reflections in above-water reflectance measurements. *Opt. Express* 2017, 25, A742–A761.
- [14] Zibordi, G., Holben, B., Slutsker, I., Giles, D., D’Alimonte, D., Melin, F., Berthon, J.-F., Vandemark, D., Feng, H., Schuster, G., Fabbri, B. E., Kaitala, S., and Seppala, J.: AERONET-OC: a network for the validation of Ocean Color primary radiometric products, *J. Atmos. Oc. Technol.*, 26, 1634–1651, 2009
- [15] Brando, V., Lovell, J, King, E., Boadle, D., Scott, R., Schroeder, T. (2016) The Potential of Autonomous Ship-Borne Hyperspectral Radiometers for the Validation of Ocean Color Radiometry Data, Remote Sensing, 2016.

- [16] ZhongPing Lee, Yu-Hwan Ahn, Curtis Mobley, and Robert Arnone. (2010). Removal of surface-reflected light for the measurement of remote-sensing reflectance from an above-surface platform. OPTICS EXPRESS. 6 December 2010 / Vol. 18, No. 25 / 26313-26324
- [17] Wernand M.R. Guidelines for (Ship-Borne) Auto-Monitoring of Coastal and Ocean Colour. In: Ackleson S.G., Trees C., editors. Proceedings of Ocean Optics XVI; Santa Fe, NM, USA. 18– 22 November 2002; <http://melia.nioz.nl/phptoweb/colors/documentation/colours38.htm>
- [18] Hommersom, A., Kratzer, S., Laanen, M. L., Ansko, I., Ligi, M., Bresciani, M., ... Peters, S. W. M. (2012). Intercomparison in the field between the new WISP-3 and other radiometers (TriOS Ramses, ASD FieldSpec, and TACCS). Journal of Applied Remote Sensing, 6, 06315-1-06315-21. DOI: 10.1117/1.JRS.6.063615
- [19] Gons, H.J., Ebert, J. & Kromkamp, J. (1998). Optical teledetection of the vertical attenuation coefficient for downward quantum irradiance of photosynthetically available radiation in turbid waters. Aquat. Ecol., 31, 299-311.
- [20] Gons, H. J. (1999) Optical teledetection of chlorophyll a in turbid inland waters. Environmental Science & Technology, 33, 1127–1132.
- [21] Rijkeboer M., Pasterkamp R. Peters S. (1999): Voorbereidende studie voor de implementatie van een spectroradiometrische veldmeetmethode voor het monitoren van optische waterkwaliteitsparameters. Report O-99/09, December 1999, IVM/VU Amsterdam
- [22] Simis, Stefan & Ruiz-Verdu, Antonio & Gómez, Jose & Peña-Martinez, Ramón & Peters, Steef & Gons, Herman. (2007). Influence of phytoplankton pigment composition on remote sensing of cyanobacterial biomass. Remote Sensing of Environment. 106. 414-427.
- [23] S.G.H. Simis and J. Olsson, "Unattended processing of shipborne hyperspectral reflectance measurements" Remote Sens. Environ., 135, 202-212, (2013).



[Page intentionally left blank]

